

# Cosmological parameters from combining the Lyman- $\alpha$ forest with CMB, galaxy clustering and SN constraints

Uroš Seljak,<sup>1,2</sup> Anže Slosar,<sup>3</sup> and Patrick McDonald<sup>4</sup>

<sup>1</sup>*Department of Physics, Princeton University, Princeton NJ 08544, U.S.A.*

<sup>2</sup>*International Center for Theoretical Physics, Trieste, Italy*

<sup>3</sup>*Faculty of Mathematics and Physics, University of Ljubljana, Slovenia*

<sup>4</sup>*Canadian Institute for Theoretical Astrophysics, University of Toronto, ON M5S 3H8, Canada*

(Dated: November 26, 2024)

We combine the Ly- $\alpha$  forest power spectrum (LYA) from the Sloan Digital Sky Survey (SDSS) and high resolution spectra with cosmic microwave background (CMB) including 3-year WMAP, and supernovae (SN) and galaxy clustering constraints to derive new constraints on cosmological parameters. The existing LYA power spectrum analysis is supplemented by constraints on the mean flux decrement derived using a principle component analysis for quasar continua, which improves the LYA constraints on the linear power. We find some tension between the WMAP3 and LYA power spectrum amplitudes, at the  $\sim 2\sigma$  level, which is partially alleviated by the inclusion of other observations: we find  $\sigma_8 = 0.85 \pm 0.02$  compared to  $\sigma_8 = 0.80 \pm 0.03$  without LYA. For the slope we find  $n_s = 0.965 \pm 0.012$ . We find no evidence for the running of the spectral index in the combined analysis,  $dn/d\ln k = -(1.5 \pm 1.2) \times 10^{-2}$ , in agreement with inflation. The limits on the sum of neutrino masses are significantly improved:  $\sum m_\nu < 0.17\text{eV}$  at 95% ( $< 0.32\text{eV}$  at 99.9%). This result, when combined with atmospheric and solar neutrino mixing constraints, requires that the neutrino masses cannot be degenerate,  $m_3/m_1 > 1.3$  (95% c.l.). Assuming a thermalized fourth neutrino we find  $m_s < 0.26\text{eV}$  at 95% c.l. and such neutrino cannot be an explanation for the LSND results. In the limits of massless neutrinos we obtain the effective number of neutrinos  $N_\nu^{\text{eff}} = 5.3_{-0.6}^{+0.4+2.1+3.8}$  and  $N_\nu^{\text{eff}} = 3.04$  is allowed only at 2.4 sigma. The constraint on the dark energy equation of state is  $w = -1.04 \pm 0.06$ . The constraint on curvature is  $\Omega_k = -0.003 \pm 0.006$ . Cosmic strings limits are  $G\mu < 2.3 \times 10^{-7}$  at 95% c.l. and correlated isocurvature models are also tightly constrained.

PACS numbers: 98.80.Jk, 98.80.Cq

## I. INTRODUCTION

The latest WMAP results of cosmic microwave background (CMB) temperature and polarization anisotropies from 3 years of observations have presented a remarkably clear view of the universe in its early epoch around redshift 1100 [1, 2]. These data, combined with other tracers such as galaxy clustering and supernovae, can be satisfied within a simple cosmological model in which the universe is filled with cold dark matter and dark energy and the initial conditions are generated through a process like inflation [3]. One of the main new results from this analysis relative to the 1st year WMAP analysis [4] is the reduced value of the optical depth due to reionization, which follows from a more sophisticated modeling and better statistics of CMB polarization data. Many other parameters are affected by this change, such as a reduced value of the amplitude of fluctuations  $\sigma_8$  and increased evidence for a red spectral index of primordial fluctuations,  $n_s < 1$  (note, however, that the optical depth constraint accounts for only part of the change in parameters).

To increase the statistical power of constraints the WMAP team added other tracers, such as small scale CMB [5, 6, 7, 8], galaxy clustering from 2dF and SDSS [9, 10, 11], supernovae [12, 13] and weak lensing [14, 15]. All of the tracers used in their analysis trace large scale

structure on scales above ten megaparsecs. However, there are many physically motivated models that can only be distinguished using small scale information. One is the running of the spectral index,  $\alpha = dn/d\ln k$ . Inflation generically predicts that there should be no running at the observable level in the current data. Therefore, any detection of running would be a major surprise and would force us to either accept models of inflation with an unusual shape of the potential with large third derivative or abandon it in favor of a better theory. In the latest WMAP analysis the data are marginally better fitted with non-zero running,  $\alpha = -0.06 \pm 0.03$ , but this analysis did not include small scale information, so the error is large.

Another class of models where small scale clustering information helps are those with massive neutrinos. These suppress power in dark matter clustering on small scales because of their free streaming, which erases their own fluctuations on scales below the free streaming length. This in turn slows down the growth of cold dark matter structure on the same scales, leaving an imprint in the dark matter power spectrum. For the relevant range of neutrino masses below 1eV the full extent of the suppression happens on megaparsec scales. From atmospheric and solar neutrino mixing detections we know that at least one neutrino has mass above 0.05eV and another above 0.01eV [16, 17], but these experiments only tell us the mass difference squared and cannot provide the

absolute scale for neutrino mass. Cosmological observations weigh neutrinos and can provide an absolute scale for their mass. Thus cosmological observations can answer one of the most important issues in neutrino physics today, the nature of the mass hierarchy of neutrinos.

It is clear that to improve upon these constraints one should determine the fluctuation amplitude on smaller scales than probed by CMB, galaxies or weak lensing. Nonlinear evolution prevents one from obtaining useful information at  $z = 0$ , so one must look for probes at higher redshift. Of the current cosmological probes, the Ly- $\alpha$  forest (LYA) – the absorption observed in quasar spectra by neutral hydrogen in the intergalactic medium (hereafter IGM) – has the potential to give the most precise information on small scales [18]. It probes fluctuations down to megaparsec scales at redshifts 2–4, so nonlinear evolution, while not negligible, has not erased the primordial information.

Currently the most precise measurement of the LYA power spectrum comes from the analysis of more than 3000 spectra from the Sloan Digital Sky Survey [19, 20]. This data set is almost two orders of magnitude larger than available previously and has dramatically reduced the errors on the amplitude and slope of the power spectrum around wave-vector  $k \sim 1h\text{Mpc}^{-1}$ . Combining this and a small amount of higher resolution Ly- $\alpha$  forest data [19, 21] with other probes has already been demonstrated to significantly improve the constraints on the running and neutrino masses [22]. For the running the current constraint from WMAP 1st year and LYA is  $\alpha = -0.003 \pm 0.010$ , which is nearly a factor of 3 improvement over the WMAP 3 year analysis without LYA. For neutrino mass the constraints including LYA are  $\sum m_\nu < 0.3 - 0.4\text{eV}$  at 95% confidence level [22, 23] in the most restrictive 6 parameter analysis.

The previous joint LYA and WMAP first year analysis in [22] suffered a significant increase in the errors on the amplitude and slope of the power spectrum from the Ly- $\alpha$  forest due to projecting out all of the poorly known nuisance parameters such as the temperature-density relation, flux of UV radiation and its fluctuations, filtering length, effects of galactic winds etc. The largest part of this increase is due to a partial degeneracy between the mean flux decrement determined by the intensity of the UV background and the amplitude of the power spectrum [18, 19]. While this degeneracy is partially broken by the flux power spectrum information itself, the error on the amplitude increases significantly over the case where the mean flux decrement was known.

One can improve upon this by providing external constraints on the redshift evolution of the mean flux decrement. In principle, if one knew the shape of the quasar spectrum, one would extract the decrement simply by comparing the actual flux level to the predicted flux level in the absence of absorption. One way to determine the continuum level of quasars is to identify regions with no absorption, but this is difficult at redshifts above 2.5, where the amount of absorption is significant and such

regions are rare. Another way is to assume quasar spectra all have the same shape and the continuum is known from observations at lower redshifts where absorption is negligible. In practice the quasars do not all have the same shape, so this approach has to be generalized. One can use the fact that the quasar continuum follows well defined variations and, identifying these at rest wavelengths longer than  $1216\text{\AA}$ , where there is no absorption, predict the shape in the Ly- $\alpha$  forest. A formalization of this procedure, including the errors, can be done by applying the principal component analysis (PCA) on the measured spectra, possibly including those measured at low redshifts where there is little Ly- $\alpha$  forest observed [24]. This procedure leads to a better determination of the mean flux decrement as a function of redshift up to an overall amplitude, which cannot be determined with this method. However, at low redshifts the level of absorption is sufficiently low that the continuum can be determined simply by connecting regions of no absorption, especially when using high resolution spectra [21]. This method therefore provides external information on the mean flux decrement, which can be used in the joint analysis.

The procedure described above has been applied to SDSS data and results presented in [19]. They show a remarkable agreement between the PCA and power spectrum based determination of the mean flux decrement as a function of redshift. This agreement provides additional confidence in the results obtained from the power spectrum analysis. Since the PCA method gives somewhat smaller errors on the mean flux decrement one can use these as external constraints to better determine the amplitude of the power spectrum. In the current analysis the improvement is modest, 20-30% on both amplitude and slope, because we do not have a tight constraint on the overall normalization of the mean absorption. The purpose of this paper is to apply these LYA constraints to the joint cosmological analysis with other data sets, including the new WMAP 3 year data. An independent analysis of similar type has recently been performed by [25].

## II. ANALYSIS

We combine the constraints from the Ly- $\alpha$  forest (LYA) [19] with the SDSS galaxy clustering analysis (SDSSgal) [10], SDSS luminous red galaxy constraints on the acoustic peak (SDSS BAO) [11], 2dF galaxy clustering analysis (2dF) [9], Gold sample of supernovae from [12] and SNLS supernovae sample [13], CMB power spectrum temperature and polarization observations from WMAP 3 year analysis (WMAP3) [1, 2] and from smaller scale experiments, including Boomerang-2k2 [8], CBI [5], VSA [6], and ACBAR [7] (CMBsmall). Contrary to the WMAP approach we do not include the SDSS bias constraints [26] nor weak lensing constraints [14], because their statistical power is weak when the LYA power spectrum is included and we prefer not to cloud the interpre-

tation of the results. We mention however that both of these constraints prefer higher normalization of  $\sigma_8$  than the recent WMAP3 results and provide additional support for the results found in this paper. Moreover, for the case of weak lensing, the recent detection of intrinsic alignment [27] may push the weak lensing normalization even further up from existing numbers, which do not account for this effect.

Our most general cosmological parameter space is

$$p = (\omega_b, \omega_{\text{dm}}, \Omega_k, \theta, \tau, f_\nu, N_\nu^{\text{eff}}, w, A, n_s, \alpha, r, A_{\text{iso}}, G\mu), \quad (1)$$

where  $\omega_b = \Omega_b h^2$ , with  $\Omega_b$  baryon density in units of the critical density,  $\omega_{\text{dm}} = \Omega_{\text{dm}} h^2$  with  $\Omega_{\text{dm}}$  dark matter density in units of the critical density,  $h$  is the Hubble's constant in units of  $100 \text{ km s}^{-1} \text{ Mpc}^{-1}$ ,  $\Omega_k = 1 - \Omega_{\text{tot}}$ , where  $\Omega_{\text{tot}}$  is the total density of the universe in units of the critical density,  $\theta$  is the angular scale of the acoustic horizon,  $\tau$  is the optical depth to the surface of last scattering,  $f_\nu$  is the fraction of dark matter in neutrinos (the rest is assumed to be cold dark matter),  $N_\nu^{\text{eff}}$  is the the energy density in relativistic background expressed in units of massless neutrino families and  $w$  the equation of state of dark energy, (which in general can be time dependent, but in this paper we only explore it as a constant). Parameters  $A_{\text{iso}}$  and  $G\mu$  describe the iso-curvature modes and string contribution (see section III I). The power spectrum of primordial fluctuations is assumed to be of the form

$$P_i(k) = A \left( \frac{k}{k_0} \right)^{n_s + \alpha \log(k/k_0)/2},$$

with the pivot point chosen to be  $k_0 = 0.05/\text{Mpc}$ . We use two additional amplitude parameterizations, which are derived parameters:  $\sigma_8$  is the rms of fluctuations in the linear density field smoothed at  $8h^{-1}\text{Mpc}$  scale at  $z = 0$ , and  $\Delta^2(k = 0.009s/\text{km}, z = 3)$  describing the fluctuations at roughly one megaparsec scale at  $z = 3$ . Finally,  $r$  is the ratio of tensor to scalar power spectrum amplitude at pivot point  $k_0$ .

We begin the exploration with the simplest 6 parameters ( $p = \omega_b, \omega_{\text{dm}}, \theta, \tau, A, n_s$ ) and then proceed by adding additional parameters, one at a time. We have tested the analysis using two independent Monte Carlo Markov Chain (MCMC) codes. The first code is described in the previous analysis of the Ly- $\alpha$  forest [22] and uses CMBFAST [28]. The second is the standard CosmoMC package [29] using CAMB [30]. We find a very good agreement between the two codes. We also compare our results whenever possible to the WMAP analysis, finding very good agreement in the analysis of WMAP data. We find some small discrepancies when other data sets are combined with WMAP. For example, in our WMAP+SDSSgal analysis we find  $\sigma_8 = 0.803$  compared to 0.772 in the WMAP paper [3], which we suspect can be explained by the different treatment of nonlinear effects in the SDSSgal data, as discussed below.

For galaxy surveys we adopt a somewhat more conservative approach in the modeling of nonlinear effects than what was done previously. The nonlinear biasing effects are argued to be well described by the expression given in [9],

$$P_{\text{gal}}(k) = b^2 \frac{1 + Qk^2}{1 + A_g k} P_{\text{lin, dm}}(k). \quad (2)$$

We use this expression with  $A_g = 1.4$  and marginalize over the bias parameter  $b$ , but rather than adopting a fixed value for  $Q$  we treat it as a free parameter. For the 2dF power spectrum we adopt a Gaussian prior  $Q = 4.6 \pm 1.5$ , as found in [9]. For the SDSS galaxy power spectrum we use the same approach with  $Q = 10 \pm 5$  and  $Q > 0$ . We use a higher mean value for  $Q$  because the SDSS data were analyzed in real space, where nonlinear effects are stronger and the value  $Q = 10$  fits well the standard nonlinear power spectrum from N-body simulations (at a percent level). Exploring the allowed range of  $Q$  in numerical simulations we found that even values above 20 are possible in real space. Therefore, we argue that using a fixed value for  $Q$  is not justified given the uncertainties in the nonlinear galaxy biasing. Instead we allow for a wider range of  $Q$  to account for the uncertainty and let the data choose the best value. In both cases we use the data up to  $k = 0.15h/\text{Mpc}$ , so the nonlinear effects are small, but not negligible.

For baryonic oscillations (BAO) we use the recent measurements of the baryonic peak in the Luminous Red Galaxies sample from the SDSS as published in [11]. To compare theoretical power spectra with the measured correlation function, we follow the prescription of the authors of the data: first we interpolate between the linear power spectrum and the “no-wiggle” equivalent using the weighting function  $\exp(-(ak)^2)$  with  $a = 7h^{-1}\text{Mpc}$ . For the “no-wiggle” spectrum we took either the approximation from [31] (as used in [11]) or the convolution with suitable top-hat in the  $\log P(k)$ - $\log k$  space. This is because the approximation of [31] is not available for all cosmological models. We also compared the results to those found when this step is ignored. In general we find that the effects from these different treatments on the final results are below one sigma, but when this is not the case we explicitly discuss it. Then the non-linear corrections are applied using the HaloFit [32] package. The resulting power spectrum is converted to the corresponding correlation function. Finally, the redshift space distortion and non-linear bias effects are accounted for by multiplying the correlation function  $\xi(r)$  by  $(1 + 0.06/(1 + (0.06h/\text{Mpc} \times r)^6))^2$ , in agreement with N-body simulations. This correlation function is then compared with the measurement using the full covariance between errors. The amplitude of the correlation function is marginalized over.

parameter	ALL DATA	ALL DATA - LYA
$\omega_b$	$0.0230^{+0.0006+0.0011+0.0017}_{-0.0006-0.0011-0.0019}$	$0.0224^{+0.0007+0.0012+0.0018}_{-0.0006-0.0013-0.0019}$
$\omega_{dm}$	$0.117^{+0.003+0.005+0.007}_{-0.002-0.005-0.008}$	$0.114^{+0.003+0.006+0.009}_{-0.003-0.005-0.008}$
$h$	$0.705^{+0.013+0.025+0.038}_{-0.013-0.023-0.038}$	$0.703^{+0.013+0.025+0.037}_{-0.013-0.028-0.037}$
$\tau$	$0.108^{+0.010+0.039+0.063}_{-0.010-0.043-0.069}$	$0.077^{+0.014+0.045+0.083}_{-0.015-0.046-0.064}$
$n_s$	$0.964^{+0.012+0.025+0.037}_{-0.012-0.026-0.038}$	$0.951^{+0.013+0.027+0.041}_{-0.013-0.027-0.041}$
$\sigma_8$	$0.847^{+0.022+0.042+0.070}_{-0.022-0.045-0.062}$	$0.798^{+0.030+0.059+0.083}_{-0.030-0.053-0.075}$
$r$	$< 0.22 (< 0.37)$	
$\alpha$	$-0.015^{+0.012+0.023+0.036}_{-0.012-0.021-0.029}$	
$N_\nu^{\text{eff}}$	$5.3^{+0.4+2.1+3.8}_{-0.6-1.7-2.5}$	
$\sum m_\nu$	$< 0.17\text{eV} (< 0.32\text{eV})$	
$m_s$	$< 0.26\text{eV} (< 0.43\text{eV})$	
$\Omega_k$	$-0.003^{+0.0060+0.0109+0.0157}_{-0.0061-0.0122-0.0180}$	
w	$-1.040^{+0.063+0.124+0.178}_{-0.063-0.130-0.208}$	
$A_{\text{iso,bar}}$	$-0.06^{+0.18+0.35+0.50}_{-0.18-0.34-0.55}$	
$A_{\text{iso,CDM}}$	$-0.007^{+0.034+0.068+0.110}_{-0.035-0.067-0.104}$	
$G\mu$	$< 2.3 \times 10^{-7} (< 2.9 \times 10^{-7})$	

TABLE I: Parameter constraints for the simplest 6-parameter model. Parameters below the horizontal line ( $r \dots G\mu$ ) were constrained individually, varying the basic 6 parameters and one extra parameter at a time. Limits are 1, 2 and 3 sigma; when only upper limits are given, these are at 95% and 99.9%.

### III. RESULTS

#### A. Basic cosmological parameters

Table I shows the results of the analysis with and without LYA for various parameter combinations, starting with the simplest 6 parameter model  $p = (\tau, \omega_b, \omega_{dm}, \Omega_\lambda, A, n_s)$ . For most parameters adding LYA reinforces the conclusions derived by WMAP. However, LYA prefers a high value of the normalization and as a consequence other parameters are also affected. For example, the preferred optical depth in the joint analysis increases to  $\tau = 0.11$  and the normalization increases to  $\sigma_8 = 0.85$ .

#### B. Amplitude of fluctuations: are the data sets compatible?

The parameter where there is the most tension between the analyses with and without the Ly- $\alpha$  forest is the amplitude of fluctuations. In terms of  $\sigma_8$ , in [22] this parameter was found to be  $\sigma_8 = 0.90 \pm 0.03$ , but this value was driven by the WMAP optical depth prior, as seen in Figure 1 of that paper, which suggests that for the new value  $\tau = 0.09$  one would find  $\sigma_8 = 0.84$ . In our new analysis we find  $\sigma_8 = 0.85 \pm 0.02$ , which is in a good agreement with this expectation. This should be compared to  $\sigma_8 = 0.75 \pm 0.06$  for WMAP alone and  $\sigma_8 = 0.80 \pm 0.03$  for WMAP combined with everything else in our analysis. There is some tension between the WMAP and LYA values and the most relevant question is whether this can be explained as a statistical fluctuation or as a signal of a systematic problem in the data.

The Ly- $\alpha$  forest effectively constrains only the amplitude and slope of the linear power spectrum at pivot point  $k = 0.009 \text{ s km}^{-1}$  and  $z = 3$ . Projections to other scales or redshifts are sensitive to cosmological parameters that are essentially unconstrained by the Ly- $\alpha$  forest. On the other hand, WMAP alone can make a well-controlled projection into the LYA amplitude-slope plane, so we make our comparison in this plane. Constraints from various experiments are shown in Figure 1. The top panel is for the case of no running using the basic 6 parameters. In this case WMAP data alone already provide a strong constraint in this plane. We see that LYA data prefer a higher value for the amplitude than WMAP and about the same value for the slope, but the 2-sigma contours have a considerable overlap. The agreement is improved if other probes, such as SDSS galaxy clustering, are added to WMAP data, which is also shown in the figure. In terms of differences in  $\chi^2$  between fitting for CMB+SDSSgal+SN and LYA separately versus jointly we find that a joint fit increases the total  $\chi^2$  by 3.8, also suggesting less than 2-sigma discrepancy. Finally, we see that the Ly- $\alpha$  forest constraints using only high resolution spectra [33, 34], while considerably weaker compared to our analysis, also prefer a higher normalization. Here we have taken the values given in [35], including the 15% error on the amplitude, marginalized separately in two redshift bins. We note that our own analysis of these data gives a somewhat smaller error on the amplitude and a somewhat larger error on the slope, but the basic conclusions remain the same.

The situation is similar when running is added as a parameter. One can see that WMAP3+SDSSgal+SN errors are comparable to LYA. In this case the WMAP3 data prefer large negative running, so even though their errors significantly increase in this plane, the mean value has been pulled towards lower values for both amplitude and slope and the agreement with LYA is actually slightly worse than before. Still, there is considerable overlap of 2-sigma contours. The difference in  $\chi^2$  between fitting WMAP3+SDSSgal+SN and LYA separately and jointly

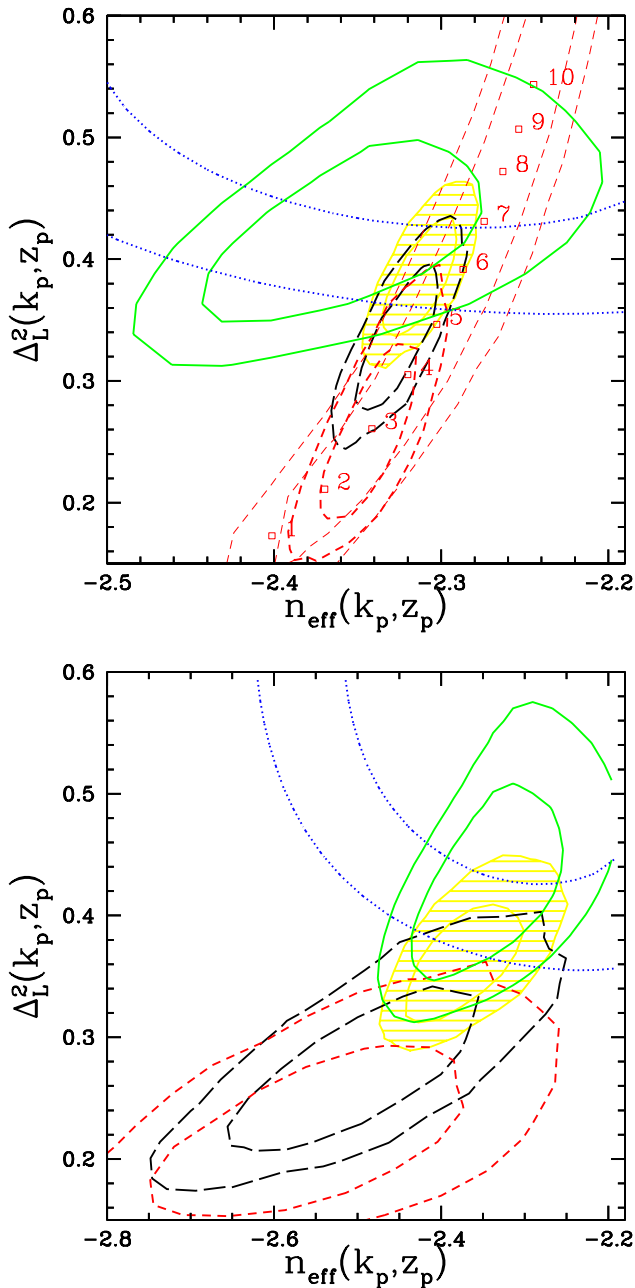


FIG. 1: Constraints on effective slope  $n_{\text{eff}}$  and amplitude  $\Delta^2$  of the linear power at  $k_p = 0.009 \text{ s/km}$ ,  $z = 3$ . The top panel corresponds to models with power-law primordial fluctuations, while the bottom includes running of the spectral index. In all cases 68% and 95% contours are shown. Red, short-dashed contours are for WMAP3, black, long-dashed for WMAP3+SDSSgal+ SN, green, solid for LYA only, and yellow, solid contours with horizontal stripes are for all of these constraints combined. The blue, dotted contours show an alternative Ly- $\alpha$  forest analysis using only high resolution spectra [35]. Top panel also shows the WMAP3 constraints when  $N_{\nu}^{\text{eff}}$  is allowed to be free (thin red short-dashed) versus being fixed at  $N_{\nu}^{\text{eff}} = 3.04$  (thick red short-dashed), as well as the central values of WMAP3 contours for different values of  $N_{\nu}^{\text{eff}}$  from 1 to 10.

is now 6.

So is there any evidence for inconsistency between WMAP3 and LYA data? From the comparisons made above it would seem that in the simplest 6-parameter models the discrepancy is around 2-sigma. However, it is important to recognize that any attempt to answer this is an a-posteriori attempt and can only provide qualitative answers. For example, if we focus on a single parameter like amplitude, which is chosen a posteriori from  $N$  parameters on the basis of the fact that it shows the most discrepancy, then we will obtain biased results: comparing two experiments in  $N$  parameters and selecting the most discrepant one on the basis of one out of  $p$  criteria (for example, if one can choose from larger than and smaller than then  $p=2$ ) will on average give one parameter in the  $1/pN$  probability corner. In our case LYA most naturally measures amplitude and slope at one megaparsec, so  $N=2$  and  $p=2$  and the statistical significance of discrepancy is further diluted by a factor of 4. Our conclusion is thus that there is no compelling evidence that the differences between LYA and WMAP3 cannot be explained as a normal statistical fluctuation and we proceed under this assumption. We return to this in the discussions.

### C. Testing inflationary models: spectral index and tensors

LYA prefers a higher amplitude at a megaparsec scale and this also pushes the primordial slope upwards. The effect is small, but relevant for the question of whether scale invariant spectrum with  $n_s = 1$  is statistically excluded. We find  $n_s = 0.965 \pm 0.012$  versus  $n_s = 0.951 \pm 0.013$  without LYA, so about one sigma change in the value. A very similar value was obtained in [36].

Adding tensors to the analysis does not improve the fit. We find

$$r < 0.22 \text{ at } 95\% \text{ c.l. } (< 0.37 \text{ at } 99.9\%), \quad (3)$$

slightly stronger than  $r < 0.28 - 0.3$  at 95% c.l. from WMAP3+SDSSgal or WMAP3+2dF analysis [3].

In Figure 2 we show the constraints in  $(n_s, r)$  plane. This plane is of interest for inflationary model builders, since many of the inflationary models can be classified according to their predictions in this plane. We see that models with  $n_s > 1$  are disfavored at  $r = 0$ , but there is a positive correlation between  $r$  and  $n_s$ .

### D. Testing inflationary models: running of the spectral index

The issue of the running of the primordial slope continues to be controversial. The latest WMAP analysis finds the strongest evidence for running so far, particularly when combined with other data sets such as small scale CMB or SDSSgal, e.g.  $\alpha = -0.066_{-0.032}^{+0.026}$  for

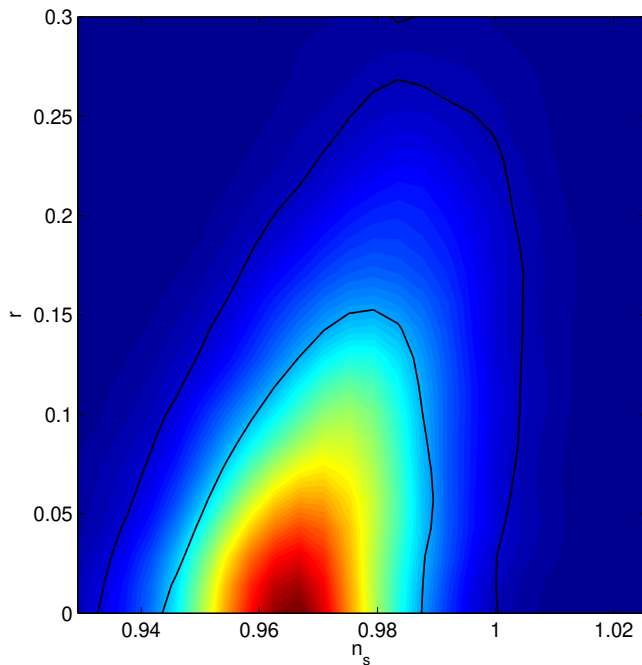


FIG. 2: This figure shows constraints on the  $n_s$ - $r$  plane. Contours enclose 68% and 95% probability.

WMAP+CBI+VSA. The dynamic range of scales is limited by CMB and galaxy clustering, and the corresponding error is large. It was previously shown that the error is significantly reduced when SDSS LYA and WMAP first year data were combined, giving  $\alpha = -0.003 \pm 0.010$  [22].

Here we redo the analysis using the new WMAP3 data and our LYA analysis. Together with all the other data we find

$$\alpha = -0.015^{+0.012+0.023+0.036}_{-0.012-0.021-0.029} \quad (4)$$

The combined analysis therefore continues to show no evidence for running, in agreement with theoretical expectations from inflation. The errors are improved relative to the WMAP 3 year analysis without LYA, but have not improved relative to LYA + first year WMAP, which also did not show any evidence for running. At this point, a conservative conclusion is that the results of the WMAP team analysis without LYA are a statistical fluctuation which is eliminated by adding the LYA data, which are much more constraining than any combination without LYA. We note that 2-sigma deviations from the true value on one of a dozen parameters are bound to happen in almost any analysis and the above discussion of dangers of a-posteriori assessment of statistical significance also applies here.

## E. Number of relativistic neutrino families

In the standard model the main relativistic components of energy density are photons and neutrinos. Neutrinos decouple earlier than photons, which receive additional entropy transfer from electron-positron annihilation, and as a result photons are hotter than neutrinos,  $T_\nu = (4/11)^{1/3}T_\gamma$ . The neutrino contribution to the energy density is usually described in terms of an effective number of neutrino families assuming the temperature relation above. The standard model predicts  $N_\nu^{\text{eff}} = 3.04$  instead of 3 because some of the entropy transfer goes to neutrinos that are not completely decoupled by the time of electron-positron annihilation. More generally, we use  $N_\nu^{\text{eff}}$  as a parametrisation of relativistic energy density in the early universe, although it should be noted that effects of neutrinos may differ from other relativistic particles [37]. If we assume  $N_\nu^{\text{eff}}$  neutrino families then the analysis finds

$$N_\nu^{\text{eff}} = 5.3^{+0.4+2.1+3.8}_{-0.6-1.7-2.5} \quad (5)$$

We find that  $P(N_\nu^{\text{eff}} < 3.04)$  is  $8.5 \times 10^{-3}$ . If only integer values of the number of neutrinos are allowed, we find that 3 : 4 : 5 neutrinos are allowed with relative probabilities 1 :  $\sim 6.4$  :  $\sim 9.7$ . How robust is the evidence against 3 neutrino families? Adding the HST constraint [38] in the form of a Gaussian prior on Hubble's constant  $h = 0.72 \pm 0.08$  lowers  $N_\nu^{\text{eff}}$  to  $4.8^{+0.4+1.6+3.0}_{-0.5-1.4-2.1}$  (but leaves the lower 3-sigma bound largely unchanged). This is because there is a strong degeneracy between the number of relativistic degrees of freedom and the dark matter energy density, as any additional relativistic component can be compensated by additional dark matter in order to keep matter-radiation equality unchanged [39] and so strong degeneracy exists with  $h$  and  $\omega_{\text{dm}}$ . For similar reasons, the constraint is also partially sensitive to the BAO treatment. Without BAO we find that  $N_\nu^{\text{eff}} = 6.0^{+1.4+2.9+3.8}_{-1.4-2.4-3.3}$ .

Removing Lyman alpha data lowers the number to  $3.9^{+0.4+2.1+4.7}_{-0.6-1.7-2.7}$ , so the evidence is significantly weakened. However, this is with both SDSS and 2dF galaxy power spectra and there is significant variation between the two. We find that the WMAP3 data together with supernovae data and SDSS main sample galaxy data favour high  $N_\nu = 7.8^{+1.1+2.3+2.9}_{-0.7-3.2-5.4}$ , while replacing SDSS galaxy data with 2dF data favours much lower number of neutrinos:  $N_\nu^{\text{eff}} = 3.2^{+0.5+3.6+6.4}_{-1.0-2.3-3.0}$  (note that we cannot reproduce the results in Table 10 of [3], however, the implausible asymmetry of their errors suggests some problem with those results). Excluding both the 2dF and SDSS main galaxy samples from the mix of all data results in  $N_\nu^{\text{eff}} = 5.2^{+0.5+2.1+3.9}_{-0.6-1.8-2.6}$ , which is only a minor change compared to all datasets.

We can conclude that the unexpectedly large result for the number of neutrino families does not rely on a single experiment as several combinations of data favour high values of relativistic energy density, albeit with an expected lower statistical significance. However, at the



moment the evidence is strongest with the Lyman alpha data. Top panel of figure 1 shows why relaxing  $N_\nu^{\text{eff}}$  improves the fit. When the parameter increases it leads to a higher amplitude and slope in LYA plane relative to the standard value, reducing the discrepancy between LYA and WMAP3 data. This is the only parameter we have found that has this effect.

Our result of combining all datasets disfavors just three mass-less neutrinos, favouring higher numbers of neutrinos instead. Big Bang Nucleosynthesis (BBN) in general tends to favour a lower number of neutrinos. In particular, [40] obtain  $N_\nu^{\text{eff}} = 3.14_{-0.65}^{+0.70}$  from BBN data alone and  $N_\nu^{\text{eff}} = 3.24_{-0.57}^{+0.61}$  by using the CMB photon-to-baryon ratio, while [41] get limits from  $N_\nu^{\text{eff}} < 3.3$  at 95% c.l. to  $N_\nu^{\text{eff}} < 6$  and 95% c.l. depending on the details of the analysis. At the moment  $N_\nu^{\text{eff}} = 4$  is the integer number of neutrinos most compatible with the data. Higher  $N_\nu^{\text{eff}}$  is at some tension with BBN constraints, while lower  $N_\nu^{\text{eff}}$  has trouble with the datasets discussed in this paper. However, newly discovered systematic issues in various datasets might still shift values around. Finally, the possibility of a statistical fluke should not be discounted, as the standard value is within 2.4 sigma of the measured value.

### F. Massive neutrinos

As mentioned in the introduction, small scale clustering combined with large scales and CMB is a very efficient way to weigh neutrinos, since these suppress the growth of structure in CDM. One can expect that adding LYA leads to a significant improvement in the constraints. Since the Ly- $\alpha$  forest prefers a high normalization compared to the CMB and the two data sets are barely compatible with each other for massless neutrinos, adding massive neutrinos which suppresses power on the LYA scale would further increase the discrepancy and make them statistically incompatible, thus providing a tight limit on the neutrino mass. We find

$$\sum m_\nu < 0.17\text{eV at } 95\% \text{c.l. } (< 0.32\text{eV at } 99.9\%). \quad (6)$$

These results depend somewhat on the treatment of the BAO data. If smoothing of the spectrum is used the limits raise to 0.35eV at 99.9% c.l. and to 0.40eV if BAO data are not included at all. Either way, this result appears to rule out the claimed Heidelberg-Moscow experiment of neutrino-less double beta decay [42].

If we combine the constraint on the sum of the masses with the existing neutrino mixing constraints, which are  $\Delta m_{12}^2 = 8 \times 10^{-5} \text{eV}^2$  for solar and  $\Delta m_{13}^2 = 2.5 \times 10^{-3} \text{eV}^2$  for atmospheric mixing [16, 17] we find for a regular hierarchy  $m_1 \sim m_2 < 0.05 \text{eV}$  and  $m_3 < 0.07 \text{eV}$ , while for 2-sigma lower limit  $\Delta m_{13}^2 = 1.8 \times 10^{-3} \text{eV}^2$  one finds  $m_3 < 0.065 \text{eV}$ . At 2-sigma the degeneracy is thus lifted at the 30% level,  $m_3/m_1 > 1.3$ . For an inverted hierarchy one has  $m_1 \sim m_2 < 0.062 \text{eV}$  and  $m_3 < 0.045 \text{eV}$

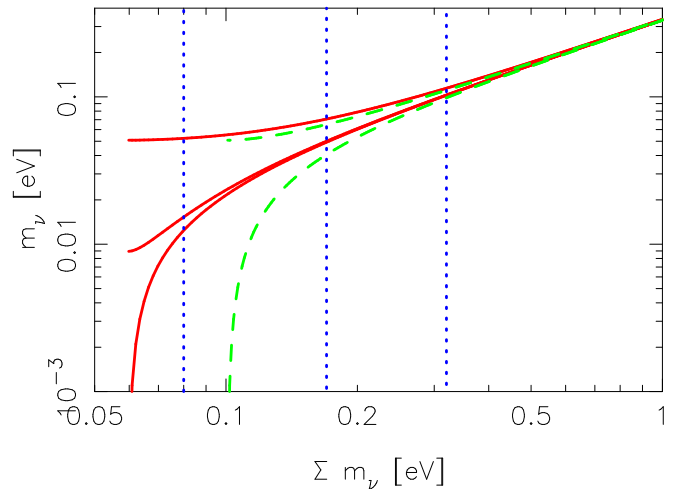


FIG. 3: This figure shows the masses of individual neutrinos plotted against the sum of masses which is constrained by the cosmological data. Solid line (red) is for normal hierarchy, while dashed (green) is for the inverted hierarchy (note that two upper to mass eigenstates are nearly degenerate in this case). Vertical dotted lines correspond to our 68%, 95% and 99.9% confidence limits. The assumed mass squared differences were taken to be  $\Delta m_{12}^2 = 8 \times 10^{-5} \text{eV}^2$  and  $\Delta m_{23}^2 = 2.5 \times 10^{-3} \text{eV}^2$ .

for  $\Delta m_{13}^2 = 1.8 \times 10^{-3} \text{eV}^2$  and again the degeneracy between  $m_1$  and  $m_3$  is lifted at the 40% level with 2-sigma confidence. This is illustrated in Figure 3.

It is interesting to note that with another factor of 2 improvement we will be able to distinguish a normal hierarchy (for which  $\sum m_\nu \sim 0.05 \text{eV}$ ) from an inverted hierarchy (with  $\sum m_\nu \sim 0.1 \text{eV}$ ), even in the limit of one massless neutrino. This is also shown in Figure 3, where the 68% confidence limit is already below the minimal inverted hierarchy solution and an inverted hierarchy is disfavored at 80% confidence. We cannot yet differentiate between these two cases in the data with any statistical significance. We also note that assuming one or the other neutrino mass makes very little difference in the estimates of other data as there are no strong degeneracies with other parameters present.

In addition to the strong evidence for mixing from solar and atmospheric neutrino experiments there is a hint for another oscillation with a much larger mass-squared difference coming from the LSND experiment [43]. This requires a mass squared difference of around  $1 \text{eV}^2$ , which cannot be incorporated in the standard 3 neutrino scheme. Of all the schemes that could incorporate this result the one that is most plausible is 3+1, three active and one sterile neutrino. However, even this scenario is strongly constrained by the short baseline oscillation experiments and the window is nearly closed at 3-sigma level [17]. Existing cosmological constraints suggest that a sterile neutrino with mass at or above 0.8eV is ruled out at 2-sigma, but not yet at 3-sigma [39]. So it is worth revisiting this issue with the new analysis.

Our new analysis considerably strengthens these limits. We find  $m_\nu < 0.26\text{eV}$  at 95% c.l. ( $0.43\text{eV}$  at 99.9%). This completely rules out a thermalized sterile neutrino with mass around  $1\text{eV}$  as the explanation for LSND experiment. However, it is possible to suppress the production of sterile neutrinos in the early universe, for example by large lepton asymmetry [44]. Therefore, there exists a possibility to accommodate these results with LSND by postulating that the neutrinos are not thermalized and their concentration is significantly suppressed relative to a thermal distribution. Note that even though the LSND-kind of sterile neutrino is disfavoured, the data in general prefer more than 3 standard neutrinos worth of relativistic species in the early universe. Thus a light sterile neutrino may well be preferred by the data, as might be other light particles.

### G. Curvature

Curvature is strongly constrained by CMB data because it determines the angular position of the acoustic feature through its effect on the angular diameter distance to the last scattering surface. However, other quantities such as the cosmological constant and matter to radiation ratio also have a similar, albeit less pronounced effect, so the CMB alone cannot determine these parameters separately with a high accuracy. Adding additional information, such as the baryonic acoustic horizon, Hubble constant or redshift-distance relation from supernovae, improves the constraints considerably. In our analysis we find

$$\Omega_k = -0.003_{-0.0061-0.0122-0.0180}^{+0.0060+0.0109+0.0157} \quad (7)$$

when curvature is added to the basic 6 parameters. This is the strongest constraint on curvature to date and the data continue to show no evidence for it. It should be noted that the curvature constraints are affected by the choice of parameters and adding some, like a time dependent equation of state, can weaken these limits considerably. On the other hand, inflation as the leading paradigm for structure formation predicts no curvature, so there is good justification to ignore it in the remaining analyses.

### H. Dark energy

Dark energy affects the rate of growth of structure, especially for  $z < 1$  where the dark energy is dynamically important. We have assumed in the analysis so far that the dark energy equation of state is  $w = -1$ . Here we relax this and explore the constraints on  $w$ . In this paper we only explore the simplest case of a constant equation of state. It has been shown in [22] that the constraints assuming a constant  $w$  are very similar to constraints obtained for time dependent  $w$  in a 3-parameter expansion

of the equation of state as a function of expansion factor, assuming these are given at redshift 0.2-0.3, the pivot point for equation of state information. So our constraint on  $w$  is more general in the sense that it remains valid for smooth time dependencies of the equation of state, assuming it is interpreted as the value at  $z=0.2-0.3$ . We find

$$w = -1.040_{-0.063-0.130-0.208}^{+0.063+0.124+0.178} \quad (8)$$

This is an improvement over other recent constraints and we see that  $w = -1$  remains very close to the best fit. Note that we have included perturbations in the dark energy both for  $w < -1$  and  $w > -1$ , although this makes very little difference in the constraints given how close the results are to  $w = -1$ , where perturbations vanish. Most of the improvement comes from the reduced error in the amplitude of fluctuations provided by the Ly- $\alpha$  forest, which helps when combined with other data sets. Our results prefer somewhat more negative values for  $w$  than the WMAP analysis [3], closer to the cosmological constant  $w = -1$ . As a result those tracker quintessence models which predict  $w \sim -0.7$  [45] appear to be strongly excluded. Other dark energy models which predict  $w \sim -1$  remain acceptable.

It is interesting to investigate the sensitivity of the constraint to the inclusion or exclusion of supernovae data. Our results above include both supernovae from the SNLS sample [13] and from the gold sample of [12]. Without the latter we find  $w = -1.05 \pm 0.07$ , while without the former we find  $w = -1.01 \pm 0.07$  and the two are statistically compatible. Finally, without any supernovae data at all the constraint is  $w = -1.02 \pm 0.12$ , so the supernovae reduce the error by a factor of two relative to the other data. In all cases cosmological constant is the preferred solution lying within one statistical deviation of the best fit value.

### I. Iso-curvature and cosmic strings

Finally, we constrain parameters of two possible extensions to the inflationary paradigm. Firstly we constrain the baryon or CDM iso-curvature modes, assuming complete correlation (or anti-correlation) and equal scale dependence of perturbations. Parameter  $A_{\text{iso}}$  is the ratio of amplitude in these fully correlated baryon/CDM iso-curvature modes to that in the adiabatic modes. We find

$$A_{\text{iso,bar}} = -0.06_{-0.18-0.34-0.55}^{+0.18+0.35+0.50} \quad (9)$$

$$A_{\text{iso,CDM}} = -0.007_{-0.035-0.067-0.104}^{+0.034+0.068+0.110} \quad (10)$$

This is about a factor of 2 better than previous limits [46]. For models predicting baryon isocurvature perturbations correlated with scalar perturbations from inflation the predictions for  $A_{\text{iso,bar}}$  are to be of order unity [47], which is severely constrained by the data. Curvaton model induced  $A_{\text{iso,CDM}}$  give a larger range of possibilities, some of which remain viable even with the new data and corresponding analyses [46].



We also constrain the amount of cosmic strings allowed by the present data. We predict a cosmic string power spectrum using calculations in [48, 49, 50], for a set of their fiducial cosmological and string network parameters. The only free parameter is the string tension  $G\mu$  which accounts for a simple quadratic scaling in amplitude. We find that the present data require

$$G\mu < 2.3 \times 10^{-7} \text{ at } 95\% \text{ c.l. } (< 2.9 \times 10^{-7} \text{ at } 99.9\%). \quad (11)$$

This is comparable to other recent limits [49, 51], but is subject to several uncertainties in the string network evolution, which may affect the relation between string tension and CMB amplitude.

#### IV. DISCUSSION AND CONCLUSIONS

In this paper we combine the current Ly- $\alpha$  forest constraints from SDSS, supplemented by a small amount of high resolution data, with the constraints from other cosmological tracers, such as galaxy clustering, supernovae and CMB, including the recent 3 year WMAP analysis. Our Ly- $\alpha$  forest analysis is an improvement over the analysis presented in [19]. The main change is the inclusion of the mean flux constraints (presented in [19] but not used in the main power spectrum analysis) derived from a principal component analysis of quasar spectra, which allows one to identify the continuum level of quasars up to an overall amplitude by using the information from about 10,000 quasar spectra. These constraints are in remarkable agreement with those derived from the power spectrum analysis, providing additional support for the consistency of the overall picture of the Ly- $\alpha$  forest. When the two are combined the resulting constraints on the amplitude and slope improve by about 20-30%.

When adding this Ly- $\alpha$  forest information to other probes we find significant improvements on many of the parameters. For the running of the spectral index we find  $\alpha = -0.015 \pm 0.012$ , compared to  $\alpha = -0.06 \pm 0.03$  without the Ly- $\alpha$  forest. Our new value is in a good agreement with the previous analysis prior to WMAP3 data [22] and in both cases provides no support for running of the spectral index being non-zero. Our results are also in agreement with a similar analysis in [25].

The most dramatic improvements are found for neutrino masses. This is expected, since the Ly- $\alpha$  forest is one of the few tracers of small scale power that is able to determine the amplitude of fluctuations in dark matter on small scales, where massive neutrinos suppress the growth of structure. For the first time the constraints are sufficiently strong that, when combined with atmospheric and solar neutrinos, they lift the degeneracy of neutrino masses at the 30% level. The current constraints are beginning to distinguish between a normal and inverted hierarchy in the limit of zero mass for the lowest mass neutrino, with the inverted hierarchy being disfavored at 80% confidence. Finally, we see no evidence for a fourth

massive neutrino that would explain the LSND experiment. The upper limit on its mass is 0.26eV at 95% confidence limit, which rules out the entire range of parameter space for the LSND experiment, assuming these neutrinos were thermalized in the early universe. On the other hand, a massless thermalized sterile neutrino is favored, since we find  $N_\nu^{\text{eff}} = 5.3_{-0.6-1.7-2.5}^{+0.4+2.1+3.8}$ .

Adding Ly- $\alpha$  forest data to the mix favors the simplest possible model without running, massive neutrinos, strings, isocurvature perturbations, curvature or dark energy equation of state different from -1. The only exception is the number of relativistic degrees of freedom, where the data prefer additional contribution beyond photons and 3 neutrino families. In many cases LYA brings the value of the parameters closer to the expected value than the analysis without LYA. As discussed in this paper, there is some tension between the Ly- $\alpha$  forest and CMB in the amplitude of fluctuations, but the statistical significance is small and the two data sets are compatible in amplitude at  $\sim 2$ -sigma. Any statistical assessment of compatibility must also take into account the a-posteriori nature of the comparison, since the data are measuring several parameters and one should not focus only on the most discrepant one to assess compatibility. It is worth mentioning that the amplitude tension of the two data sets is at a similar level of significance as the evidence for running or curvature in the WMAP data, which many (especially inflation theorists) would be willing to accept as a statistical fluctuation until proven otherwise. This is expected: one is estimating a dozen parameters and it is not surprising if some are 2-sigma away from their true values. In fact, the evidence for running is eliminated after Ly- $\alpha$  forest data is added and the error is reduced by a factor of 2-3. So one can either accept that the original evidence was a statistical fluctuation which was settled conclusively with Ly- $\alpha$  forest and other data, or one can argue that some of these data have issues with systematic errors and should be excluded from the analysis. In this paper we have proceeded under the assumption that these are just normal statistical fluctuations and that the data are compatible with each other. Future observations and investigations of possible systematic effects will provide a more definitive answer.

We wish to conclude with a brief discussion of the role of unaccounted systematics in the current cosmological analyses. No cosmological probe is completely immune to systematic uncertainties and all must be subject to ongoing investigations, as well as cross-checks among different data sets. The remarkable progress in statistical precision of cosmological data over the past few years has been unprecedented, but often the improved statistics of the data sets has not been adequately matched by correspondingly improved analysis of systematic errors. To some extent this is expected: systematic errors are more difficult to track down and quantify and a detailed analysis of these can take years, so is often done after the initial results have been published. However, such analysis is necessary and provides important confidence in the

results. A lot of progress has been made on this front in the past years and in some cases these concerns have been lessened after a detailed study of systematic errors has been published. A case in point is the remarkably detailed analysis of systematics in the recent WMAP 3 year data, which has strengthened the reliability of cosmological constraints derived from WMAP data. It is essential that corresponding investigations are done with other tracers as well and we believe that there is some room for improvement in many cases. For some cosmological tracers, such as supernovae and weak lensing, the open issues (e.g. intrinsic alignments and shear calibration in weak lensing, calibration and evolution in SN) are known and well organized campaigns to address them are underway. For other tracers, such as galaxy clustering, uncertainties in galaxy formation already limit the statistical power that can be extracted on small scales, but the full extent of this uncertainty needs to be quantified better.

Since the key results of this paper depend crucially on the reliability of the Ly- $\alpha$  forest it is particularly important to address the systematics of this tracer. Recent investigations of the Ly- $\alpha$  forest have shown that possible astrophysical complications are either small or can be incorporated into the analysis [52, 53, 54, 55]. Moreover, an independent analysis of the SDSS flux power spectrum obtained results that are in agreement with the original analysis [56], although a somewhat lower amplitude is favored [25] (note that one does not expect exactly the same result because [56] used only SDSS data, while we add high resolution data that helps break parameter degeneracies). However, there are remaining worries about possible other effects that have not yet been thought of and more investigations are needed to exhaust the list of possibilities.

One area where progress in Ly- $\alpha$  forest is expected

soon is in numerical simulations. The original analysis in [19] used an indirect approach patching together several simulations with differing box sizes to cover the whole dynamical range in observations and relying on hydro-PM simulations calibrated by only a few fully hydrodynamic simulations to cover the relevant range of parameter space. With the fast hydrodynamic codes optimized for the Ly- $\alpha$  forest that are available today, such as Enzo [57] or the Eulerian moving frame TVD+PM code described in [58], this is no longer necessary and parameter space can be covered entirely with hydrodynamic simulations. In addition, a code comparison project focusing on Ly- $\alpha$  forest is underway and will address the issue of agreement among different hydrodynamic codes.

We expect that as the progress in statistical precision of cosmological constraints slows down in the future more emphasis will be given to the investigation of systematic errors. Until then the current cosmological constraints obtained from combining many different cosmological probes, including the ones presented in this paper, should be viewed as preliminary. However, the fact that the different tracers agree with each other within the range of normal statistical fluctuations bodes well for the current round of analyses and suggests systematic effects may be subdominant.

We thank Alexey Makarov for help with the MCMC code and we acknowledge use of CAMB, CMBFAST and CosmoMC packages, as well as LAMBDA supported by NASA office of Space Science. Some computations were performed on CITA's McKenzie cluster which was funded by the Canada Foundation for Innovation and the Ontario Innovation Trust [59]. U.S. is supported by the Packard Foundation, NASA NAG5-1993 and NSF CAREER-0132953. AS is supported by the Slovenian Research Agency grant Z1-6657.

- 
- [1] G. Hinshaw, M. R. Nolta, C. L. Bennett, R. Bean, O. Dore', M. R. Greason, M. Halpern, R. S. Hill, N. Jarosik, A. Kogut, et al., ArXiv Astrophysics e-prints (2006), arXiv:astro-ph/0603451.
  - [2] L. Page, G. Hinshaw, E. Komatsu, M. R. Nolta, D. N. Spergel, C. L. Bennett, C. Barnes, R. Bean, O. Dore', M. Halpern, et al., ArXiv Astrophysics e-prints (2006), arXiv:astro-ph/0603450.
  - [3] D. N. Spergel, R. Bean, O. Dore', M. R. Nolta, C. L. Bennett, G. Hinshaw, N. Jarosik, E. Komatsu, L. Page, H. V. Peiris, et al., ArXiv Astrophysics e-prints (2006), arXiv:astro-ph/0603449.
  - [4] C. L. Bennett, M. Bay, M. Halpern, G. Hinshaw, C. Jackson, N. Jarosik, A. Kogut, M. Limon, S. S. Meyer, L. Page, et al., *Astrophys. J.* **583**, 1 (2003).
  - [5] A. C. S. Readhead, B. S. Mason, C. R. Contaldi, T. J. Pearson, J. R. Bond, S. T. Myers, S. Padin, J. L. Sievers, J. K. Cartwright, M. C. Shepherd, et al., *Astrophys. J.* **609**, 498 (2004).
  - [6] C. Dickinson, R. A. Battye, P. Carreira, K. Cleary, R. D. Davies, R. J. Davis, R. Genova-Santos, K. Grainge, C. M. Gutiérrez, Y. A. Hafez, et al., *Mon. Not. R. Astron. Soc.* **353**, 732 (2004).
  - [7] C.-L. Kuo, P. Ade, J. J. Bock, M. D. Daub, J. Goldstein, W. L. Holzapfel, A. E. Lange, M. Newcomb, J. B. Peterson, J. Ruhl, et al., *American Astronomical Society Meeting* **201** (2002).
  - [8] C. J. MacTavish, P. A. R. Ade, J. J. Bock, J. R. Bond, J. Borrill, A. Boscaleri, P. Cabella, C. R. Contaldi, B. P. Crill, P. de Bernardis, et al. (2005), arXiv:astro-ph/0507503.
  - [9] S. Cole, W. J. Percival, J. A. Peacock, P. Norberg, C. M. Baugh, C. S. Frenk, I. Baldry, J. Bland-Hawthorn, T. Bridges, R. Cannon, et al., *Mon. Not. R. Astron. Soc.* **362**, 505 (2005).
  - [10] M. Tegmark, M. R. Blanton, M. A. Strauss, F. Hoyle, D. Schlegel, R. Scoccimarro, M. S. Vogeley, D. H. Weinberg, I. Zehavi, A. Berlind, et al., *Astrophys. J.* **606**, 702 (2004).
  - [11] D. J. Eisenstein, I. Zehavi, D. W. Hogg, R. Scoccimarro,

- M. R. Blanton, R. C. Nichol, R. Scranton, H.-J. Seo, M. Tegmark, Z. Zheng, et al., *Astrophys. J.* **633**, 560 (2005).
- [12] A. G. Riess, L. Strolger, J. Tonry, S. Casertano, H. C. Ferguson, B. Mobasher, P. Challis, A. V. Filippenko, S. Jha, W. Li, et al., *Astrophys. J.* **607**, 665 (2004).
- [13] P. Astier, J. Guy, N. Regnault, R. Pain, E. Aubourg, D. Balam, S. Basa, R. G. Carlberg, S. Fabbro, D. Fouchez, et al., *Astron. Astrophys.* **447**, 31 (2006).
- [14] L. Van Waerbeke, Y. Mellier, and H. Hoekstra, *Astron. Astrophys.* **429**, 75 (2005).
- [15] U. Seljak, A. Makarov, R. Mandelbaum, C. M. Hirata, N. Padmanabhan, P. McDonald, M. R. Blanton, M. Tegmark, N. A. Bahcall, and J. Brinkmann, *Phys. Rev. D* **71**, 043511 (2005).
- [16] Y. Ashie et al. (Super-Kamiokande), *Phys. Rev. D* **71**, 112005 (2005), hep-ex/0501064.
- [17] M. Maltoni, T. Schwetz, M. A. Tortola, and J. W. F. Valle, *New J. Phys.* **6**, 122 (2004), hep-ph/0405172.
- [18] R. A. C. Croft, D. H. Weinberg, N. Katz, and L. Hernquist, *Astrophys. J.* **495**, 44 (1998).
- [19] P. McDonald, U. Seljak, R. Cen, D. Shih, D. H. Weinberg, S. Burles, D. P. Schneider, D. J. Schlegel, N. A. Bahcall, J. W. Briggs, et al., *Astrophys. J.* **635**, 761 (2005).
- [20] P. McDonald, U. Seljak, S. Burles, D. J. Schlegel, D. H. Weinberg, R. Cen, D. Shih, J. Schaye, D. P. Schneider, N. A. Bahcall, et al., *Astrophys. J. Supp.* **163**, 80 (2006).
- [21] P. McDonald, J. Miralda-Escudé, M. Rauch, W. L. W. Sargent, T. A. Barlow, R. Cen, and J. P. Ostriker, *Astrophys. J.* **543**, 1 (2000).
- [22] U. Seljak, A. Makarov, P. McDonald, S. F. Anderson, N. A. Bahcall, J. Brinkmann, S. Burles, R. Cen, M. Doi, J. E. Gunn, et al., *Phys. Rev. D* **71**, 103515 (2005).
- [23] A. Goobar, S. Hannestad, E. Mortsell, and H. Tu, *ArXiv Astrophysics e-prints* (2006), arXiv:astro-ph/0602155.
- [24] N. Suzuki, D. Tytler, D. Kirkman, J. M. O'Meara, and D. Lubin, *Astrophys. J.* **618**, 592 (2005).
- [25] M. Viel, M. G. Haehnelt, and A. Lewis (2006), astro-ph/0604310.
- [26] U. Seljak, A. Makarov, R. Mandelbaum, C. Hirata, N. Padmanabhan, P. McDonald, M. Blanton, M. Tegmark, N. Bahcall, and J. Brinkmann, *ArXiv Astrophysics e-prints* (2004), astro-ph/0406594.
- [27] R. Mandelbaum, C. M. Hirata, M. Ishak, U. Seljak, and J. Brinkmann, *Mon. Not. R. Astron. Soc.* **367**, 611 (2006).
- [28] U. Seljak and M. Zaldarriaga, *Astrophys. J.* **469**, 437 (1996).
- [29] A. Lewis and S. Bridle, *Phys. Rev. D* **66**, 103511 (2002).
- [30] A. Lewis, A. Challinor, and A. Lasenby, *Astrophys. J.* **538**, 473 (2000).
- [31] D. J. Eisenstein and W. Hu, *Astrophys. J.* **496**, 605+ (1998).
- [32] R. E. Smith, J. A. Peacock, A. Jenkins, S. D. M. White, C. S. Frenk, F. R. Pearce, P. A. Thomas, G. Efstathiou, and H. M. P. Couchman, *Mon. Not. R. Astron. Soc.* **341**, 1311 (2003).
- [33] T. . Kim, M. Viel, M. G. Haehnelt, R. F. Carswell, and S. Cristiani (2003), astro-ph/0308103.
- [34] R. A. C. Croft, D. H. Weinberg, M. Bolte, S. Burles, L. Hernquist, N. Katz, D. Kirkman, and D. Tytler, *Astrophys. J.* **581**, 20 (2002).
- [35] M. Viel, M. G. Haehnelt, and V. Springel, *Mon. Not. R. Astron. Soc.* **354**, 684 (2004).
- [36] A. G. Sanchez et al., *Mon. Not. Roy. Astron. Soc.* **366**, 189 (2006), astro-ph/0507583.
- [37] S. Bashinsky and U. Seljak, *Phys. Rev. D* **69**, 083002 (2004).
- [38] W. L. Freedman, B. F. Madore, B. K. Gibson, L. Ferrarese, D. D. Kelson, S. Sakai, J. R. Mould, R. C. Kennicutt, H. C. Ford, J. A. Graham, et al., *Astrophys. J.* **553**, 47 (2001).
- [39] S. Dodelson, A. Melchiorri, and A. Slosar, *ArXiv Astrophysics e-prints* (2005), arXiv:astro-ph/0511500.
- [40] R. H. Cyburt, B. D. Fields, K. A. Olive, and E. Skillman, *Astropart. Phys.* **23**, 313 (2005), astro-ph/0408033.
- [41] K. A. Olive and D. Thomas, *Astropart. Phys.* **11**, 403 (1999), hep-ph/9811444.
- [42] H. V. Klapdor-Kleingrothaus, I. V. Krivosheina, A. Dietz, and O. Chkvorets, *Phys. Lett.* **B586**, 198 (2004), hep-ph/0404088.
- [43] C. Athanassopoulos, L. B. Auerbach, R. L. Burman, I. Cohen, D. O. Caldwell, B. D. Dieterle, J. B. Donahue, A. M. Eisner, A. Fazely, F. J. Federspiel, et al., *Physical Review Letters* **77**, 3082 (1996).
- [44] R. Foot and R. R. Volkas, *Phys. Rev. D* **55**, 5147 (1997), hep-ph/9610229.
- [45] P. J. Steinhardt, L. Wang, and I. Zlatev, *Phys. Rev. D* **59**, 123504 (1999).
- [46] M. Beltran, J. Garcia-Bellido, J. Lesgourgues, and M. Viel, *Phys. Rev. D* **72**, 103515 (2005), astro-ph/0509209.
- [47] L. Boubekour and P. Creminelli (2006), hep-ph/0602052.
- [48] L. Pogosian and T. Vachaspati, *Phys. Rev. D* **60**, 083504 (1999), astro-ph/9903361.
- [49] L. Pogosian, I. Wasserman, and M. Wyman, *ArXiv Astrophysics e-prints* (2006), astro-ph/0604141.
- [50] U. Seljak and A. Slosar (2006), astro-ph/0604143.
- [51] A. A. Fraisse (2006), astro-ph/0603589.
- [52] P. McDonald, U. Seljak, R. Cen, P. Bode, and J. P. Ostriker, *Mon. Not. R. Astron. Soc.* **360**, 1471 (2005).
- [53] A. Meiksin and M. White, *Mon. Not. R. Astron. Soc.* **350**, 1107 (2004).
- [54] R. A. C. Croft, *Astrophys. J.* **610**, 642 (2004).
- [55] K. Lai, A. Lidz, L. Hernquist, and M. Zaldarriaga (2005), astro-ph/0510841.
- [56] M. Viel and M. G. Haehnelt, *Mon. Not. R. Astron. Soc.* **365**, 231 (2006).
- [57] B. W. O'Shea, G. Bryan, J. Bordner, M. L. Norman, T. Abel, R. Harkness, and A. Kritsuk, *ArXiv Astrophysics e-prints* (2004), astro-ph/0403044.
- [58] H. Trac and U. Pen, *New Astronomy* **9**, 443 (2004).
- [59] J. Dubinski, R. Humble, U.-L. Pen, C. Loken, and P. Martin, *ArXiv Astrophysics e-prints* (2003), arXiv:astro-ph/0305109.